*Published online 18 December 2012* *Nucleic Acids Research, 2013, Vol. 41, No. 3* ***1555–1568***
*doi:10.1093/nar/gks1273*

# Novel function of the unique N-terminal region of RUNX1c in B cell growth regulation

**Gareth Brady, Claudio Elgueta Karstegl and Paul J. Farrell***

Section of Virology, Imperial College Faculty of Medicine, Norfolk Place, London W2 1PG, UK

Received September 4, 2012; Revised November 2, 2012; Accepted November 6, 2012

## ABSTRACT

**RUNX family proteins are expressed from alternate promoters, giving rise to different N-terminal forms, but the functional difference of these isoforms is not understood. Here, we show that growth of a human B lymphoblastoid cell line infected with Epstein–Barr virus is inhibited by RUNX1c but not by RUNX1b. This gives a novel functional assay for the unique N-terminus of RUNX1c, and amino acids of RUNX1c required for the effect have been identified. Primary resting B cells contain RUNX1c, consistent with the growth inhibitory effect in B cells. The oncogene TEL–RUNX1 lacks the N-terminus of RUNX1c because of the TEL fusion and does not inhibit B cell growth. Mouse Runx1c lacks some of the sequences required for human RUNX1c to inhibit B cell growth, indicating that this aspect of human B cell growth control may differ in mice. Remarkably, a cell-penetrating peptide containing the N-terminal sequence of RUNX1c specifically antagonizes the growth inhibitory effect in B lymphoblastoid cells and might be used to modulate the function of human RUNX1c.**

## INTRODUCTION

The mammalian RUNX gene family consists of the *RUNX1*, *RUNX2* and *RUNX3* genes. They express distinct *runt* family transcription factors that differentially regulate lineage-specific gene expression in several developmental pathways (1–3). All three transcription factors have strong protein sequence similarity, particularly in the DNA-binding 'runt homology domain' (RHD), and are thought to bind similar consensus DNA sequences. Despite similar DNA binding activities, there are few functional overlaps *in vivo* as demonstrated by the highly distinct knockout phenotypes in mice (3). Part of the explanation for this lack of functional redundancy is a distinct spatiotemporal control of expression of each Runx family member that makes co-expression of two Runx genes in the same cell type unusual (4,5). However, there are likely also to be functional differences between the different RUNX proteins; this article identifies a novel growth regulation function of RUNX1 that requires the unique N-terminus of RUNX1c.

RUNX1 is the best characterized RUNX family member because of its key role in haematopoietic development. In mice, it is expressed first in the embryo during the early development of haematopoietic stem cells in the dorsal aorta where it is required for the maturation of these cells (6,7). Consistent with this, knockout mice exhibit a complete absence of definitive haematopoiesis in the liver and die at E12.5 (8). RUNX1 additionally plays key roles in adult haematopoiesis (9,10). It is also frequently translocated in lymphoid cancers where it becomes fused to *TEL* (TEL–RUNX1) in malignancies of B-cells and *ETO* (RUNX1–ETO) in myeloid leukaemia (1).

Like all RUNX gene family members, the transcription of RUNX1 occurs from two distinct promoters (Figure 1B): the P1 (distal) and the P2 (proximal) promoter (11). Expression from these promoters is tightly controlled during haematopoietic development (3) and is functionally non-redundant (12). Expression from P1 or P2 gives rise to distinct isoforms of RUNX1 derived from the first promoter-specific exons and differential splicing of the sequences encoding the N-terminal parts of the proteins. The major isoform of RUNX1 expressed from the P1 promoter is RUNX1c, whereas the major isoform expressed from the P2 promoter is RUNX1b. These proteins differ by the presence of 32 unique N-terminal amino acids in RUNX1c (Figure 1A) and 5 unique N-terminal amino acids in RUNX1b; the remaining 448 amino acids are identical in the two proteins. In RUNX3, the equivalent forms are called RUNX3$^{p46}$ (P1) and RUNX3$^{p44}$ (P2). Although some differences in biochemical activity have been observed for the two RUNX1 isoforms (13,14), a detailed analysis of how they differ functionally has not yet been possible because of lack of a model system where a clear differential activity can be demonstrated.

*To whom correspondence should be addressed. Tel: +44 20 7594 2005; Fax: +44 20 7594 3973; Email: p.farrell@imperial.ac.uk

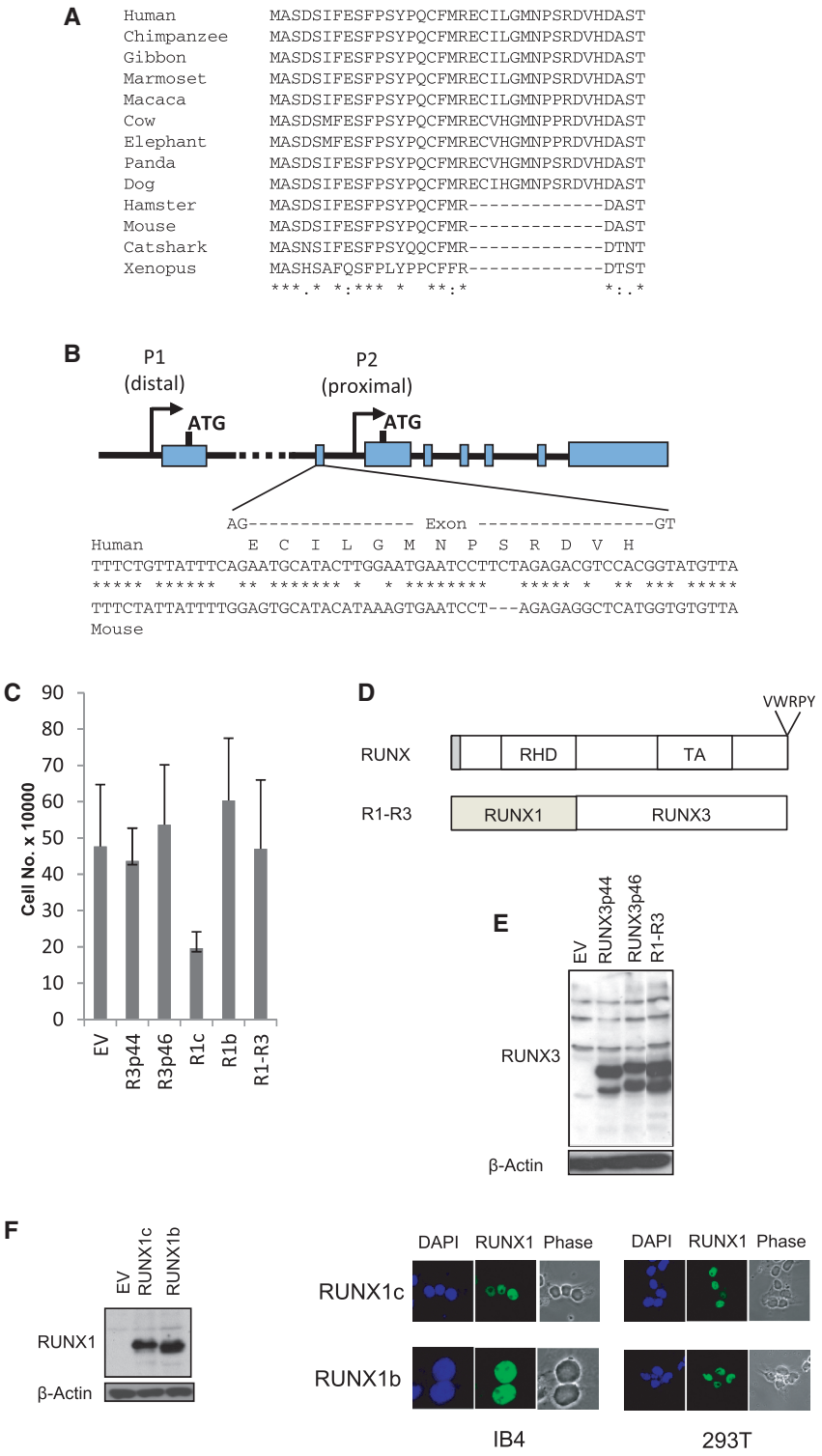


**Figure 1.** RUNX1c but not RUNX1b represses B cell proliferation. (**A**) Clustal W alignment of RUNX1c from different species. (**B**) Diagram of RUNX1 gene with an alignment of the genomic DNA sequence spanning exon 2 of human RUNX1c and the orthologous mouse RUNX1 gene sequence. Nucleotides shown are human hg19 chr21:36265209–36265270, mouse mm10 chr16:92701388–92701446. The position of exon 2 is marked above the amino acids ECILGMNPSRDVH that are encoded by exon 2. The essential AG of the $Py_nAG$ splice acceptor consensus before the start of the exon is changed to GG in the mouse sequence. (**C**) IB4 LCLs were electroporated with pCEP4 constructs expressing indicated chimera and wild-type RUNX products, then selected with hygromycin and counted after 2 weeks selection. The results presented show the average cell number from 4–6 determinations with standard deviation shown by error bars. (**D**) Diagram aligning the canonical RUNX structure with chimera R1–R3, constructed by fusion of RUNX1c amino acids 1–172 to amino acids 150–415 of $RUNX3^{p44}$. TA indicates transactivation domain, and RHD is runt homology domain (DNA binding). (**E**) Expression of RUNX3 constructs with chimera R1–R3 in HEK293T cells was detected by immunoblotting lysates and probing using an anti-RUNX3 antibody with a β-actin loading control. (**F**) RUNX1c and RUNX1b were shown to be expressed in IB4 cells by immunoblotting lysates, and both demonstrated nuclear localization in IB4 and HEK293T cells by confocal microscopy. Data are representative of four separate experiments.

We previously reported that the Epstein-Barr virus (EBV) transcription factor EBNA2 induces RUNX3$^{p44}$ on infection of resting B cells and is essential for proliferation of these cells (15,16). Resting B cells express high levels of RUNX1c, but its expression abruptly ceases after B cell activation or EBV infection. We demonstrated a key role for RUNX3$^{p44}$ in this process by repressing RUNX1c expression through direct binding of RUNX3$^{p44}$ to two RUNX consensus binding sites near the Runx1 P1 transcription start. The removal of RUNX1c by this mechanism during B cell activation was shown to be essential for proliferation of the B cells because artificial expression of RUNX1c in proliferating lymphoblastoid cell lines (LCLs) blocked cell growth (17).

We have now found that this ability of RUNX1c to prevent B cell growth specifically requires the N-terminus of RUNX1c, as RUNX1b does not cause the growth inhibition. This creates a convenient assay to define a novel functional domain within the N-terminus of RUNX1c, and we have identified the amino acids in the N-terminal domain that are required. Remarkably, a synthetic peptide corresponding to the N-terminal sequence prevents the ability of RUNX1c to inhibit B cell growth; this peptide might be used to specifically manipulate the function of RUNX1c.

## MATERIALS AND METHODS

### Plasmid construction

Unless stated, all RUNX3 and RUNX1 constructs were constructed in the pCEP4 or pMEP4 vectors (Invitrogen) inserting between the KpnI and NotI sites. Chimera R1–R3 consists of residues 1–172 of RUNX1c followed by residues 150–415 RUNX3$^{p44}$. All other vectors were reported previously (17). pCEP4–RUNX1b was constructed by polymerase chain reaction (PCR) amplification of RUNX1c from residue 33 using a forward primer with a 5′ overhanging sequence encoding the RUNX1b N-terminus (MRIP). RUNX1c truncation mutants were constructed by amplifying RUNX1c from different regions along the N-terminus. Site-directed mutants of the RUNX1c N-terminus and the DNA-binding mutant (DBM) were generated using overlapping primer sets introducing the relevant mutation with the Quickchange mutagenesis kit (Stratagene). The pMEP4-TAP-tag (TT) root vector was constructed by ligating the TAP-tag sequence between the NotI and BamHI sites of pMEP4 for fusion to the C-terminus of RUNX1 sequences. The RUNX1cΔE20–H32 splice variant was made by PCR amplifying RUNX1c starting at residue 33 (DAST) using a forward primer with an overhang containing the upstream sequence of the RUNX1c N-terminus (MASDSIFESFPSYPQCFMR). RUNX1c ΔVWRPY was generated by PCR amplifying RUNX1c coding sequence and introducing a stop codon before the VWRPY coding sequence. RUNX1 fusion cDNAs TEL–RUNX1 and RUNX1–ETO (a kind gift from Tony Ford) were sub-cloned into pCEP4. CBF-β-flag was cloned from LCL cDNA using primers CBFFP: CCCAAGCTTATGCCGCGCGTCGTGCCC and CBFRP: ATAGTTTAGCGGCCGCTCACTTGTC GTCGTCGTCCTTGTAGTCACGAAGTTTGAG GTC ATC and inserted into the HindIII and NotI sites of pBKCMV (Agilent Technologies). CBF-β was also sub-cloned into pET28A (Novagen) between the HindIII and NotI sites for recombinant expression with a Poly-His tag.

### Cell lines

DG75 (18) is an EBV-negative BL cell line. IB4 is an EBV-immortalized LCL (19). Cell lines were maintained in RPMI 1640 (Gibco-BRL) supplemented with 10% (v/v) heat-inactivated fetal calf serum, penicillin and streptomycin. Inducible cell lines were maintained in the same medium with 300 μg/ml of hygromycin. Human embryonic kidney (HEK) 293T cells were maintained in Dulbecco's modified Eagle's medium supplemented with 10% (v/v) fetal calf serum and antibiotics. The 293T cells were transfected using Genejuice (Merck).

### Immunoblotting and antibodies

Radioimmunoprecipitation assay (RIPA) lysates were prepared, and immunoblotting was performed as described (17). Where indicated, samples were normalized by cell counting then lysed and sonicated. For immunoblotting, membranes were probed with: 1/200 dilution of rabbit polyclonal antibodies (Oncogene research products), anti-AML-1 (RUNX1) RHD (Ab-2), anti-AML-2 (RUNX3) (Ab-1), 1/1000 of RUNX1 monoclonal antibody (M-201; Santa Cruz), 1/5000 of GAPDH (AM300; Ambion), 1/500 of CBF-β (PA1-317; Pierce) or a 1/5000 dilution of mouse monoclonal anti-β-actin (AC-15; Sigma). The monoclonal anti-BZLF1 antibody has been described previously (20). Secondary antibodies were horseradish peroxidase-conjugated goat anti-rabbit immunoglobulin (Sigma) or horseradish peroxidase-conjugated sheep anti-mouse immunoglobulin (Sigma). Bound immunocomplexes were detected by enhanced chemiluminescence (GE Healthcare).

### RNA extraction and reverse transcription–PCR

Total cell RNA was extracted with TRIzol (Invitrogen). Cytoplasmic RNA was extracted with the RNeasy kit and treated on the column with RNase-free DNase (Qiagen). cDNA was prepared with a Protoscript first-strand cDNA synthesis kit (New England Biolabs) using oligo(dT). To detect the expression of BLK and GAPDH, a GoTaq PCR system (Promega) was used with the following primers: BLK (TTCTTTAGATCACAGGGTCG and A GACTTCGCCGAATTGTCC) or GAPDH (TGAAGGT CGGAGTCAACGGATTG and GCCATGGAATTTGC CATGCCATGGGTGG)

### Pull-down assays

10 cm dishes of 293HEK cells transfected with RUNX1 and CBF-β plasmids or induced pMEP4–RUNX1TT cell lines were lysed with RIPA buffer. Lysates, normalized using a Bradford DC protein assay (Bio-Rad), were incubated for 4 h at 4°C with

anti-Flag-beads (Sigma), washed three times with RIPA and the beads were boiled in sample buffer for analysis by immunoblotting. Recombinant CBF-β–His was produced in BL21 *Escherichia coli* and purified using Nickel-NTA agarose (Qiagen); the beads were used for pull-down assays as described earlier in the text.

### Electrophoretic mobility shift assay

Nuclear extracts were prepared by washing cells in phosphate buffered saline (PBS), followed by re-suspension in buffer A [10 mM of HEPES pH 7.9, 1.5 mM of $MgCl_2$, 10 mM of KCl, 0.5 mM of DTT, 0.5 mM of PMSF and protease inhibitor cocktail (Boehringer Mannheim)]. Nuclei were isolated by lysing cells in buffer A containing 0.1% (v/v) of NP40 on ice for 5 min and centrifugation at 5800*g* for 30 s.

Nuclei were then lysed in buffer B (20 mM of HEPES pH 7.9, 1.5 mM of $MgCl_2$, 420 mM of NaCl, 0.2 mM of EDTA, 25% of glycerol (v/v), 1 mM of DTT, 0.5 mM of PMSF and 1× protease inhibitor cocktail) at 4°C for 15 min. Cell debris were removed by centrifugation at 11 600*g* for 10 min at 4°C, and the protein concentration was determined (Bio-Rad). Aliquots of extract were stored at −70°C. Oligonucleotides were designed against the human myeloperoxidase (MPO) promoter containing a RUNX binding site. MPOF: CTGATCACTAACCACA ACCAGTTCTGC and MPOR: CGTCTTGACCAACA CCAA TCACTAGTC were annealed and end labelled with [$\alpha^{32}$-P] dGTP using Klenow DNA polymerase. EMSA reactions were carried out in a 14 µl containing 10 mg of nuclear extract, 20 mM of HEPES pH 7.9, 0.1 M of KCl, 0.2 mM of EDTA, 20% of glycerol (v/v), 0.5 mM of PMSF, 10.5 mM of DTT, protease inhibitor cocktail, 5 µg of bovine serum albumin and 2 µg of poly (dI-dC) (Sigma) and pre-incubated with cold competitor oligonucleotides or antibodies at 25°C for 5 min if required. In total, 250 000 counts (~100 ng) of $^{32}$P-labelled probe was added, and the reaction mixture was incubated at 25°C for 30 min. Complexes were separated on a non-denaturing 4% of poly-acrylamide gel in 0.5× TBE that was then fixed in 10% of acetic acid, 45% of ethanol (v/v), dried and analysed on a phosphorimager.

### Confocal microscopy

Confocal microscopy HEK293 cells were cultured on poly-L-lysine-coated coverslips in six-well dishes at ~50% density and were transfected with 3 µg of plasmid DNA. LCLs were overlaid on to poly-L-lysine-coated coverslips and were allowed to partially air dry before fixation. Cells were fixed using 4% of paraformaldehyde and permeabilized with 0.05% of Triton X-100 in PBS. Primary anti-RUNX1 antibody (Oncogene) was diluted 1/500 in blocking buffer (PBS with 5% bovine serum albumin, 0.05% of Triton X-100), and samples were incubated overnight at 4°C with shaking. The coverslips were washed three times with blocking buffer and fluorescein isothiocyanate-conjugated anti-rabbit secondary antibody (Sigma) was applied at a 1/1000 dilution in blocking buffer. The samples were again washed in triplicate, coverslips were mounted in MOWIOL and visualized using a confocal microscope.

### Electroporation of LCLs for transient and stable expression

The $2 \times 10^6$ exponentially growing IB4 LCLs were electroporated with 5 µg of plasmid DNA using the Neon electroporation system (Invitrogen). Cells were recovered in conditioned medium into 6-well plates, and 300 µg/ml of hygromycin selection was administered on the following day. Medium containing hygromycin was replaced every 3 or 4 days until stable outgrowth was obtained. Cultures were tested for inducible protein expression using 1 µM of cadmium chloride ($CdCl_2$; Sigma). Transient cells were harvested after 2 weeks selection for analysis.

### Cell-penetrating peptides

Peptides containing the N-terminus of RUNX1c residues 1–32 followed by 9 arginine residues (R1NTCPP: MASDSIFESFPSYPQCFMRECILGMNPSRDVH RR RRRRRRR), the D4A mutation and a scrambled version of this sequence (CtrlCPP: MGLEDSSFFRQSY AVEIPISMDRMSPCFCNPH RRRRRRRRR) were obtained from Peptide Synthetics, UK. Peptides were dissolved in DMSO at 5 mM.

## RESULTS

### RUNX1c but not RUNX1b represses growth of LCLs

Comparison of RUNX1c protein sequences from different species demonstrates the conservation of the N-terminal 33 amino acids that are unique to RUNX1c (Figure 1A). The mouse and hamster Runx1c N-terminus lacks amino acids $E^{20}$–$H^{32}$ present in RUNX1c of most mammals. These amino acids are encoded by exon 2 of human RUNX1c. Although sequence similar to exon 2 is present in the mouse genome at an orthologous position in the RUNX1 gene (Figure 1B), a point change in the splice acceptor changes its essential AG to GG, most likely preventing inclusion of this exon in the mouse RUNX1c mRNA. The absence of this exon in the mRNA has been noted before (13,21).

We showed previously that resting human B cells contain RUNX1c (17). Induction of B cell proliferation by Epstein–Barr virus infection involves induction of RUNX3, which represses the expression of the RUNX1c and allows the cell proliferation. We showed that expression of RUNX1c from an artificial promoter by electroporation of an expression plasmid causes a profound decrease in the outgrowth of these cells, indicating that its removal by RUNX3 has a vital role in the proliferation or survival of activated B cells (17). Remarkably, we have now found that RUNX1b does not prevent B cell growth in this system (Figure 1C), providing a new assay for functional difference between RUNX1c and RUNX1b in human lymphoblastoid cells.

The ability of RUNX1c to repress LCL growth required sequences unique to both the N- and C-terminus of

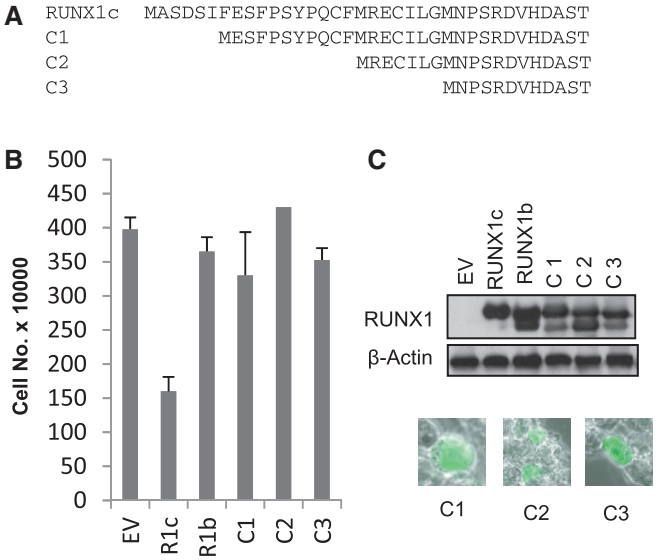


**Figure 2.** Disruption of RUNX1c N-terminus removes growth repressive activity. (**A**) Alignment of RUNX1c with truncation mutants. (**B**) The $2 \times 10^6$ IB4 LCLs were electroporated with pCEP4–RUNX1c, RUNX1b and truncations C1–3. Cells were selected with hygromycin and counted after 2 weeks selection. The results are shown as average cell number with standard deviation as error bars, as in Figure 1. (**C**) Expression of RUNX1 constructs was tested by immunoblotting lysates using a RUNX1 antibody. β-Actin served as a loading control. Confocal microscopy demonstrated that all three RUNX1c truncations C1–3 localize in the nucleus similarly to wild-type RUNX1c.

RUNX1c because chimera R1–R3, which has the N-terminus of RUNX1c but the C terminus of RUNX3, failed to inhibit LCL growth (Figure 1C and D). Expression of the RUNX proteins was checked by transient transfection into 293T cells, which do not express RUNX1 or RUNX3. The predicted proteins were observed in western blotting, and all were shown to be nuclear in an immunofluorescence assay (Figure 1E and F).

The role of the N-terminal part of RUNX1c in growth inhibition was tested directly by sequentially deleting the RUNX1c N-terminus, creating three deletion mutants C1, C2 and C3 (Figure 2A). These were expressed in IB4 LCLs in the same electroporation and hygromycin selection assay. Removal of even the first six amino acids (C1) was sufficient to prevent the growth repressive activity of RUNX1c (Figure 2B). The deletion mutants localized in 293T and IB4 cells similarly to RUNX1c and were expressed at similar levels (Figure 2C). These data show that deletion of even a small section of the RUNX1c N-terminus disrupts the growth repression function.

### The RUNX1c growth repressive activity can be linked to specific residues within the N-terminus

Our experiments so far on RUNX1c growth inhibition were performed using a transient electroporation LCL outgrowth assay. The small scale of this technique and substantial cell death of untransfected cells in the hygromycin selection hinder further analysis. We, therefore, developed a conditional system in which stably transfected lymphoblastoid cell lines could be induced to express RUNX1 alleles. RUNX1c and RUNX1b were cloned under the control of a metallothionein-regulated promoter using the pMEP4 plasmid. A C-terminal TAP-tag motif was added to the RUNX1c and RUNX1b sequences for these experiments.

This system was found to accurately demonstrate the differential effect of RUNX1c and RUNX1b on cell growth. Cadmium chloride ($CdCl_2$) induction of RUNX1c caused a decrease in the proliferation of IB4 cells, but induction of RUNX1b did not have this effect (Figure 3A). We examined the DNA content of cells over the duration of this time course, and although RUNX1c did not seem to have a significant effect on any particular stage of the cell cycle, there was a significant increase in the sub G1 peak at 5 days induction, implying cell death was present at later stages (Figure 3B). There was, however, no significant increase in PARP cleavage on induction of RUNX1c (data not shown). Growth inhibition by RUNX1c thus seems to be complex and affects multiple stages of the cell cycle. The expression level of RUNX1c induced by $CdCl_2$ in the LCLs was similar to that observed in the latency I BL cell line DG75 and so can be considered to be physiologically normal (Figure 3C).

To determine which residues are required for the growth repressive activity of RUNX1c, alanine scanning mutants of all the RUNX1c N-terminal residues from $S^3$ to $H^{32}$ were prepared by site-directed mutagenesis. Stably transfected IB4 cell lines of all 30 mutants were tested in a growth assay with or without 5 days of treatment with $CdCl_2$. RUNX1c mutants were expressed at comparable levels and could be divided into three categories (Figure 4A). The first category was residues whose mutations had little or no effect on RUNX1c growth repression and were, therefore, not required for its activity ($S^3$, $I^6$, $F^{10}$, $Y^{13}$, $P^{14}$, $Q^{15}$, $C^{16}$, $M^{18}$, $R^{19}$, $M^{25}$, $R^{29}$ and $D^{30}$). The second category of mutants was partially required for RUNX1c activity ($S^5$, $E^8$, $S^9$, $P^{11}$, $S^{12}$). The third category was residues whose mutation abolished the activity of RUNX1c, and, therefore, are required ($D^4$, $F^7$, $F^{17}$, $E^{20}$, $C^{21}$, $I^{22}$, $L^{23}$, $G^{24}$, $N^{26}$, $P^{27}$, $S^{28}$, $V^{31}$, $H^{32}$). Some of these point mutants were also tested in the transient assay (without the TAP-tag). The mutants selected behaved in a similar fashion to their stable inducible, TAP-tagged equivalents with approximately equivalent levels of expression (Figure 4B). Although there was some variation in expression level, this was not related to the ability to inhibit cell growth in these assays.

The TAP-tag in the inducible IB4 cell lines also allowed testing for possible novel stable protein interactions dependent on the N-terminus of RUNX1c. The inducible RUNX1c and RUNX1b TAP-tagged lines were compared in large-scale pull-down experiments, analysing the pull-down material by mass spectrometry. Although the association of endogenous CBF-β with both RUNX1 isoforms was confirmed, we did not detect any proteins that reproducibly interacted differentially with RUNX1c compared with RUNX1b (data not shown). This approach would have only detected a stable interaction of proteins off DNA in free solution, but the result suggests that a more subtle effect of the N-terminus on

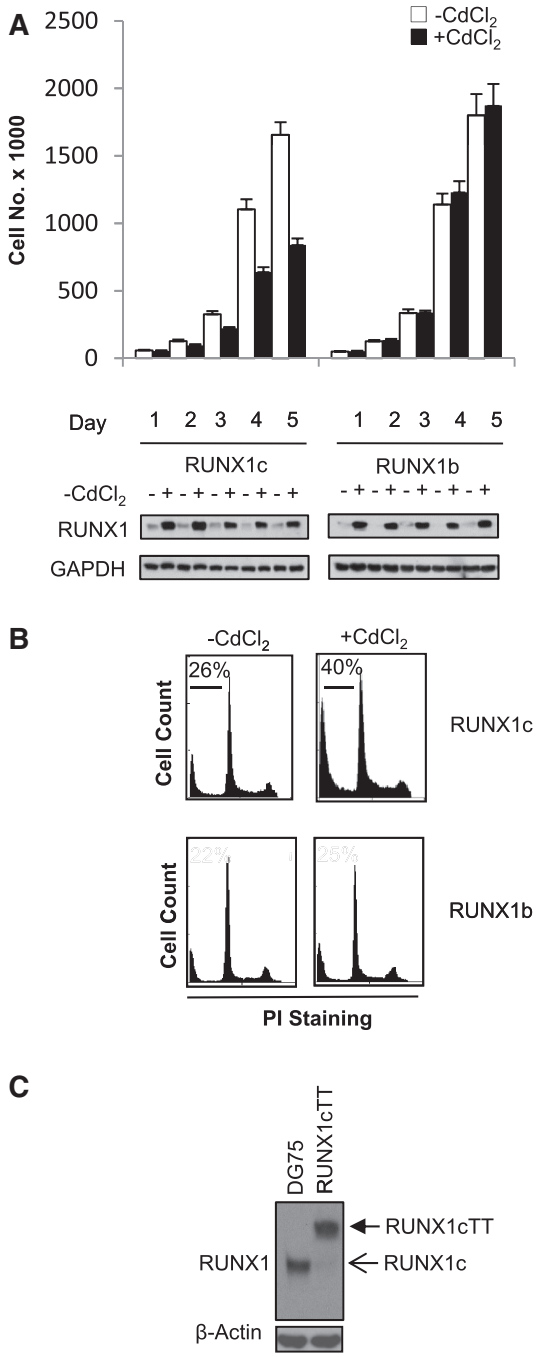


**Figure 3.** Inducible stable RUNX1c TAP-tagged IB4 cell line reconstitutes growth inhibitory activity (**A**). Inducible IB4 pMEP4 stable cell lines expressing RUNX1cTT and RUNX1bTT were seeded at $1 \times 10^5$ per ml in six-well dishes induced with 1 μM of $CdCl_2$ and were counted over 5 days of culture. The results presented show the average cell number from 4–6 determinations with standard deviation as error bars. Expression from RUNX1 constructs was tested by immunoblotting lysates using a RUNX1 antibody. GAPDH was used as a loading control. (**B**) Cells were harvested at day 5 post-induction, fixed in 70% (v/v) of ethanol and stained with 50 μg/ml of propidium iodide (Sigma) containing ribonuclease A (Sigma). DNA content was then examined by flow cytometry. Percentage sub-diploid DNA content is shown. (**C**) Comparison of RUNX1c proteins levels in lysates from DG75 cells and IB4 pMEP4–RUNX1cTT induced with 1 μM of $CdCl_2$ after immunoblotting and probing with an anti-RUNX1 monoclonal antibody (A-2). β-Actin was the loading control.

RUNX1 function is a more likely explanation for the differential activity.

### Human–mouse differences, DNA binding and the VWRPY motif

Reverse transcription (RT)–PCR of RNA from mouse spleen or thymus using primers spanning exon 1 to exon 4 confirmed that mice express only the recognized RUNX1c RNA form lacking exon 2 and encoding $\Delta E^{20}$–$H^{32}$ protein (data not shown). A stable IB4 inducible cell line expressing a TAP-tagged human RUNX1c splice variant lacking exon 2 (N-terminus equivalent to mouse RUNX1c) was produced (Figure 5A) and tested in the growth assay. As predicted from the point mutagenesis, the $E^{20}$–$H^{32}$ exon 2 deletion mutant did not inhibit LCL growth (Figure 5B) despite a similar level of expression to the full-length RUNX1c (Figure 5C). In mouse B cells, there is no equivalent of the EBV-infected human B lymphoblastoid line to allow homologous testing of mouse RUNX1c (lacking exon 2), but it seems likely from these data that there is a difference in the function of RUNX1c between human and mouse B cells.

A DNA binding mutant (DBM) of RUNX1c was prepared by mutating $R^{161}$ to a Glycine, a natural mutation known to disrupt DNA binding of RUNX1b (22). In the transient outgrowth assay in IB4 cells, the DBM failed to repress growth, although it showed correct sub-cellular localization in 293T and IB4 cells (Figure 6A).

Earlier experiments (Figure 1C) had shown a requirement for the C-terminus of RUNX1c for growth repression that could not be provided by the C-terminus of RUNX3. We further examined the requirement for regions C-terminal of the RHD by generating $CdCl_2$-inducible cell lines expressing a truncated form of RUNX1c containing sequences from the start of the protein to the end of the RHD (RUNX1cNT), the equivalent form of RUNX1b (RUNX1bNT) and a form lacking either the 1c or 1b N-terminus (RUNX1NT). These cell lines inducibly expressed high levels of RUNX1 product (Figure 6B, right panel). Interestingly, all three proteins displayed strong nuclear localization, although significant, diffuse cytoplasmic localization was also evident (Figure 6B). These truncated RUNX proteins lack the known C-terminal nuclear localization motif of RUNX1 (23), but they do contain the minimal DNA-binding domain, which may result in diffuse localization with partial nuclear tropism as we observe. RUNX1cNT and the other mutant forms failed to repress LCL growth (Figure 6B, left panel), indicating that sequences C-terminal of the RHD are required for the growth inhibition.

The extreme C-terminus contains the VWRPY sequence, through which TLE family transcriptional repressors are recruited (24,25). The VWRPY deletion mutant (RUNX1cΔVWRPY) repressed the growth of the IB4 cells to a similar extent as RUNX1c (Figure 6C), indicating that it is not required for the growth repressive activity of RUNX1c in this context. It, therefore, seems that, in addition to the N-terminus and the DNA-binding domain, RUNX1 sequences C-terminal of the RHD and

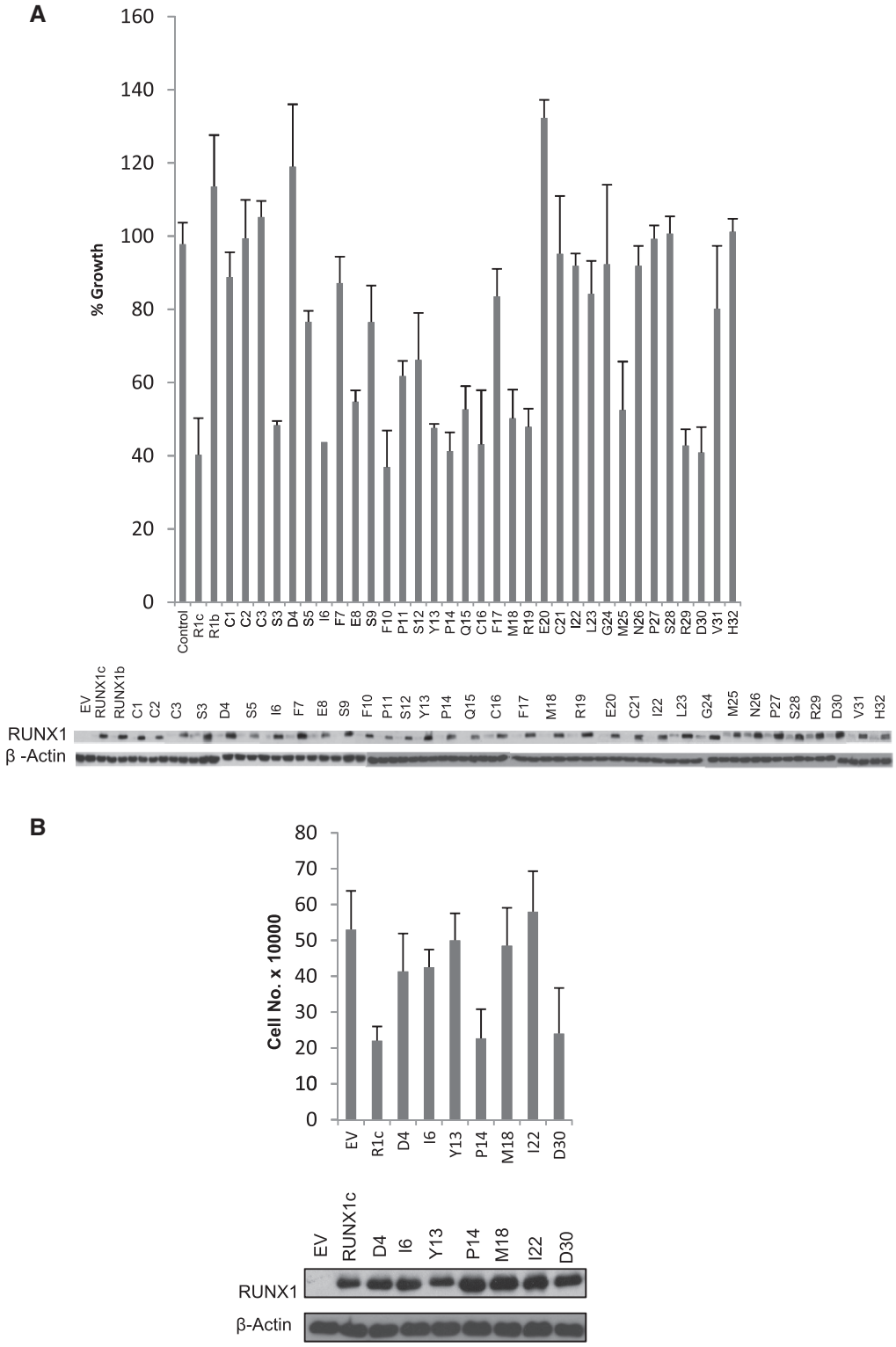


**Figure 4.** RUNX1c growth inhibitory activity requires specific residues within the unique N-terminus. (**A**) IB4 cell lines containing pMEP–RUNX1cTT with the indicated N-terminal mutations were seeded at $1 \times 10^5$ per ml in six-well dishes, induced with 1 μM of $CdCl_2$ and counted after 5 days culture. Mutations converted the indicated original amino acid to alanine. The results are presented as average percentage growth of induced cells compared with non-induced cells from triplicate samples with standard deviation from 4–6 determinations for each cell line. Cells with and without 1 μM of $CdCl_2$ were lysed in sample buffer after 5 days and immunoblotted for RUNX1c expression (shown below) with a β-actin loading control. (**B**) Transient electroporation of $2 \times 10^6$ IB4 cells with 5 μg of pCEP–RUNX1c and selected site-directed mutants. Cells were selected with hygromycin and counted after 2 weeks outgrowth. The results presented show the average cell number and standard deviation as error bar, determined as earlier in the text. Cells were lysed in sample buffer after 2 weeks and immunoblotted for RUNX1c expression, using β-actin as a loading control. Data are representative of at least three separate experiments.

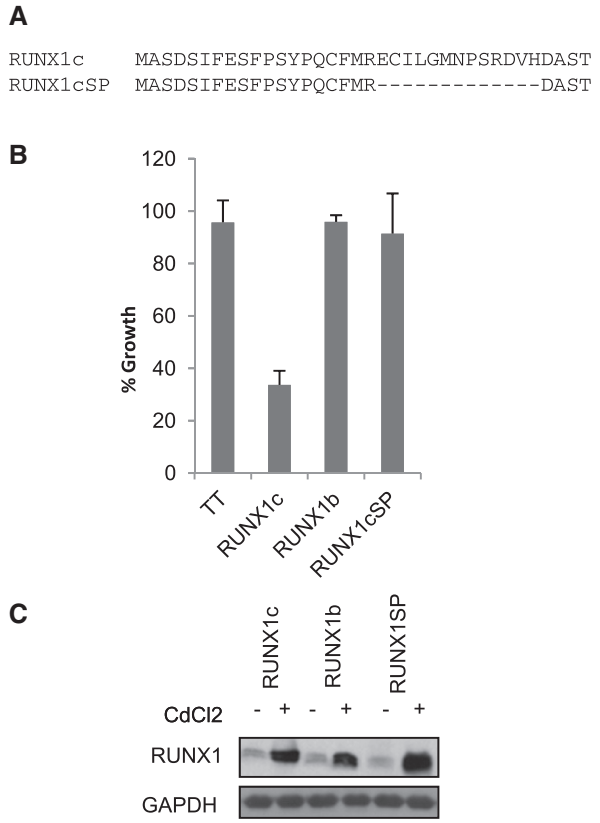


**Figure 5.** Human RUNX1c lacking residues E20–H32 missing from murine RUNX1c does not inhibit cell growth. (**A**) Protein sequence alignment of RUNX1c and RUNX1cΔ E20–H32 murine-like N-terminal splice form (RUNX1cSP). (**B**) Inducible IB4 pMEP4 stable cell lines expressing TT vector alone, RUNX1cTT, RUNX1bTT and RUNX1cSP were seeded at $1 \times 10^5$ per ml in six-well dishes induced with 1 μM of $CdCl_2$ and counted after 5 days culture. The results are presented as average percentage growth of induced cells compared with non-induced cells from six determinations with standard deviation shown as error bars. Cells were then lysed in sample buffer and immunoblotted for detection of RUNX1 levels with a GAPDH loading control. Data are representative of three separate experiments.

unique to RUNX1 (but not the VWRPY sequence) are required for the ability to inhibit B cell proliferation.

As the DBM mutant of RUNX1 (Figure 6A) that cannot bind DNA did not inhibit B cell growth, it is likely that growth inhibition is mediated through specific gene regulation by RUNX1. At present, we do not know the key genes involved in this. There does not seem to be a general difference in gene regulation because testing a known RUNX1 target gene BLK showed no difference in expression levels in the B cell system in response to expression of RUNX1c or RUNX1b (Figure 6D). To test whether there is a simple difference in the ability to bind specifically to DNA, RUNX1c and RUNX1b were tested in an electrophoretic mobility shift assay (EMSA) using the known RUNX1-binding site in the MPO gene (Figure 1E). LCL extracts could not be used for this experiment because of the large amount of endogenous RUNX3; therefore, RUNX1c or RUNX1b were expressed by transfection in 293 cells, which contain endogenous CBF-β but no RUNX1 or RUNX3. Nuclear extracts were prepared and shown to have equal amounts of RUNX1 protein (Figure 6E, lower panel). The EMSA (Figure 6E, upper panel) showed a specific RUNX1 complex (arrowed), which was competed by an excess of the same non-radioactive DNA sequence but not by a non-specific competitor. There was no significant difference between RUNX1c and RUNX1b in the amount of complex formed (Figure 6E). This was not a consequence of the assay being saturated, as twice as much nuclear extract gave an increased amount of EMSA complex.

### Differential effect of RUNX1 fusion oncogenes on LCL growth

TEL–RUNX1 is unable to repress the growth of LCLs (17), consistent with its activity as a B cell-specific oncogene. The absence of the N-terminus of RUNX1c in TEL–RUNX1 might thus be relevant to the ability of this type of translocation to cause B cell tumours. To test whether loss of growth repression was a general property of RUNX1 fusion oncogenes in this system, TEL–RUNX1 or RUNX1–ETO were expressed in the transient transfection LCL outgrowth assay. TEL–RUNX1c gave a slight, yet consistent, increase in cell numbers but RUNX1–ETO inhibited the outgrowth as effectively as RUNX1c (Figure 7). Although RUNX1–ETO showed strong nuclear localization like RUNX1c, TEL–RUNX1 was predominantly localized in the cytoplasm both in 293T cells and IB4 cells, perhaps explaining its inability to inhibit B cell growth, irrespective of any contribution from the absence of the N-terminal sequences specific to RUNX1c.

The inhibition of cell growth caused by RUNX1–ETO probably occurs by a different mechanism to that of RUNX1c because RUNX1–ETO has a RUNX1b N-terminus. Ectopic expression of RUNX1–ETO in early haematopoietic development gave rise to myeloid or granulocytic but not lymphocytic cells expressing RUNX1–ETO (26–28); mutagenesis of these mice gave rise to myeloid malignancies (29). This suggests that, not only is its expression in B cells not tolerated, it preferentially leads to malignancy with a myeloid specificity. Conversely, the opposite is true for TEL–RUNX1 (30,31). It, therefore, appears that the activity of these oncogenic forms of RUNX1 may differ from the specific mechanism by which RUNX1c inhibits normal B cell proliferation.

### RUNX1c and RUNX1b bind CBF-β equally

Although we found no difference in DNA binding (Figure 6E), previous research showed that RUNX1c binds to consensus RUNX sites somewhat more strongly than RUNX1b in gel shift assays (13). An analogous difference in distal and proximal form binding was demonstrated for RUNX2 (32). Both these studies used murine RUNX1c lacking the $E^{20}$–$H^{32}$ region required for growth modulating activity in human B cells; therefore, this *in vitro* differential binding activity does not explain our observations on cell growth. The DNA binding affinity of the RUNX family is modulated through the binding of CBF-β, which increases RUNX DNA

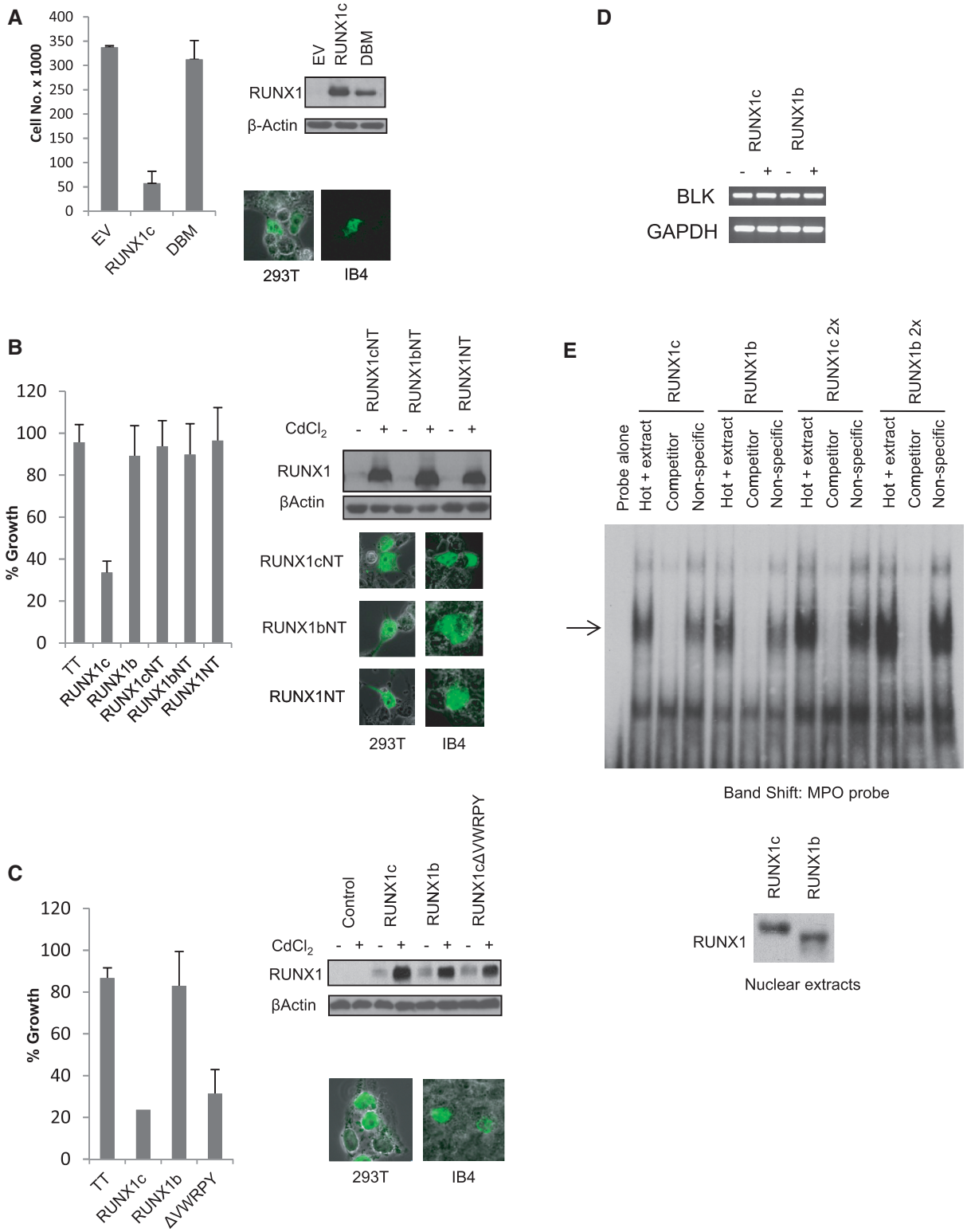


**Figure 6.** RUNX1c proliferation block requires DNA binding and the transactivation domain but is VWRPY independent. (**A**) The $2 \times 10^6$ IB4 cells were electroporated with 5 μg of pCEP4–RUNX1c or the RUNX1c DBM, then selected with hygromycin and counted after 2 weeks selection. The results presented show the average cell number from six deteminations with standard deviations shown as error bars. Cells were then lysed in sample buffer and immunoblotted for detection of RUNX1 levels and for β-actin as a loading control. Localization of the RUNX1c DBM protein by confocal microscopy demonstrated its targeting to the nucleus as wild-type RUNX1c. (**B**) IB4 pMEP4 stable cell lines inducibly expressing TT vector alone, RUNX1cTT, RUNX1bTT and truncated forms of RUNX1 were seeded at $1 \times 10^5$ per ml in six-well dishes, induced with 1 μM of $CdCl_2$ and counted after 5 days culture. The truncated forms of RUNX1 comprised the N terminal portion of each isoform to the end of the RHD (RUNX1cNT and RUNX1bNT). RUNX1NT lacked either N-terminus, starting from sequence DAST. The results are presented as average percentage growth of induced cells compared with non-induced cells from six determinations with standard deviation shown as error bars. A portion of

(continued)

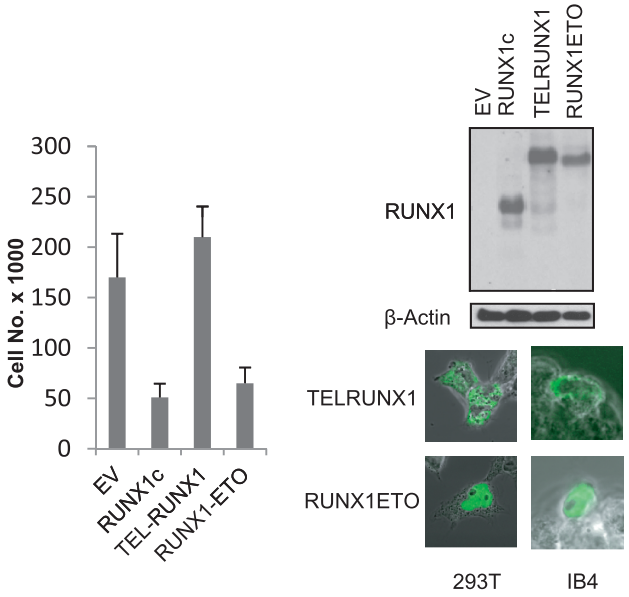


**Figure 7.** The RUNX1 oncogenic fusions TEL–RUNX1 and RUNX1–ETO also exhibit differential effects on B cell proliferation. The $2 \times 10^6$ IB4 LCLs were electroporated with 5 μg of pCEP4–RUNX1c, pCEP4–TEL–RUNX1 or pCEP4–RUNX1–ETO, then selected with hygromycin and counted after 2 weeks selection. The results presented show the average cell number as aforementioned with standard deviations shown as error bars. Cells were then lysed in sample buffer and immunoblotted for detection of RUNX1 protein levels, using β-actin as a loading control. Immunofluorescence microscopy of the RUNX1c proteins was performed to determine their localization in HEK293T cells and LCLs. Data are representative of three separate experiments.

binding by ~3-fold (33–35). We, therefore, examined the relative ability of the RUNX1 isoforms to bind CBF-β. CBF-β cDNA was cloned by RT-PCR from LCL cDNA and was engineered to have either a FLAG tag or a His tag on the C-terminus. The CBF-β–His was expressed in *E. coli* and affinity purified on Nickel resin beads. The ability of this CBF-β–His to associate with RUNX1c and RUNX1b was tested using a pull down assay with extracts either from transfected 293T cells (Figure 8A) or from the inducible IB4 LCLs (Figure 8B). No difference was observed between the ability of RUNX1c and RUNX1b to associate with CBF-β.

Additionally, the CBF-β–FLAG expression plasmid was co-transfected with RUNX1c or RUNX1b expression plasmids into 293T cells, and immunoprecipitation was performed with anti-FLAG antibody. Co-transfection of RUNX1b with CBF-β caused an overall decrease in the levels of both proteins (Figure 8C and D) but RUNX1c did not show this effect with CBF-β. No such reduction in the level of RUNX1b was observed when it was co-expressed with a control protein, the EBV BZLF1 transcription factor, in the same vector (Figure 8D). These data indicate that CBF-β and RUNX1b have a specific ability to mutually destabilize each other when acutely expressed in 293 cells. It is difficult to dismiss this as an over-expression phenomenon because of the specificity of the effect to the RUNX1b–CBF-β combination. However, when we examined the levels of CBF-β in the inducible IB4 LCLs with and without induction of RUNX1c or RUNX1b, no such destabilization was observed (Figure 8E). Differential CBF-β binding or destabilization, therefore, does not seem to be an explanation for the differences in RUNX1c and RUNX1b activity on cell growth observed in the LCLs.

### A cell permeable peptide containing the RUNX1c N-terminus prevents the RUNX1c growth inhibition

The ability of cell permeable peptides (CPPs) to pass the membrane and be bio-available inside cells is provided by the nine arginine residues added to the C-terminus (36,37). Comparing a RUNX1c N-terminal CPP and a control scrambled sequence CPP (Figure 9A), we found that the RUNX1c CPP specifically prevented the ability of RUNX1c to inhibit cell growth (Figure 9B) while not affecting the levels of the inducible RUNX protein in these cells. The ability of the RUNX1c CPP to prevent cell growth inhibition by RUNX1c was also abolished by introducing the D4A point mutation into the peptide (Figure 9C), corresponding to the mutagenesis shown earlier. For this experiment, the peptides were re-synthesized and were tested several times to confirm the ability to specifically prevent RUNX1c from inhibiting LCL cell growth. This peptide competition might in principle be used to manipulate RUNX1c function in lymphoblastoid cells *in vivo*.

## DISCUSSION

Although they only differ by the N-terminal 33 amino acids, we show here a clear difference in the regulation of cell growth and survival between RUNX1c and RUNX1b in human B cells. RUNX1c is the main form found in the lymphoid compartment, whereas RUNX1b is chiefly expressed in myeloid lineages (13). RUNX1c in human resting B cells is repressed when RUNX3$^{p44}$ expression

**Figure 6.** Continued
the cells was then lysed in sample buffer and immunoblotted for detection of RUNX1 levels, also using β-actin as a loading control. Some of the cells were also used for localization of truncated RUNX1 forms by confocal microscopy. (**C**) IB4 pMEP4 stable cell lines expressing Tap tag vector TT alone, RUNX1cTT, RUNX1bTT and RUNX1cΔVWRPY were seeded at $1 \times 10^5$ per ml in six well dishes, induced with 1 μM of $CdCl_2$ and counted after 5 days culture. The results are presented as average percentage growth of induced cells compared with non-induced cells as aforementioned. Cells were then lysed in sample buffer and immunoblotted for detection of RUNX1 levels with a β-actin loading control. The localization of RUNX1 forms was determined by confocal microscopy. Data are representative of three separate experiments. (**D**) IB4 stable pMEP–RUNX1cTT and RUNX1bTT cells were seeded at $1 \times 10^5$ cells per ml in six-well dishes and induced with 1 μM of $CdCl_2$. RNA was extracted after 5 days culture, cDNA was generated and RT–PCR was performed on samples for the expression of BLK and GAPDH. (**E**) The 10-cm dishes of 293T cells were transfected with 8 μg of pCEP–RUNX1c or pCEP4–RUNX1b, and nuclear extracts from these were analysed by EMSA for binding of RUNX factors using a $^{32}$P-labelled MPO oligonucleotide with cold competitor and non-specific probe controls. Western blotting was also performed on nuclear extracts to demonstrate equal loading of RUNX1 protein in EMSAs.

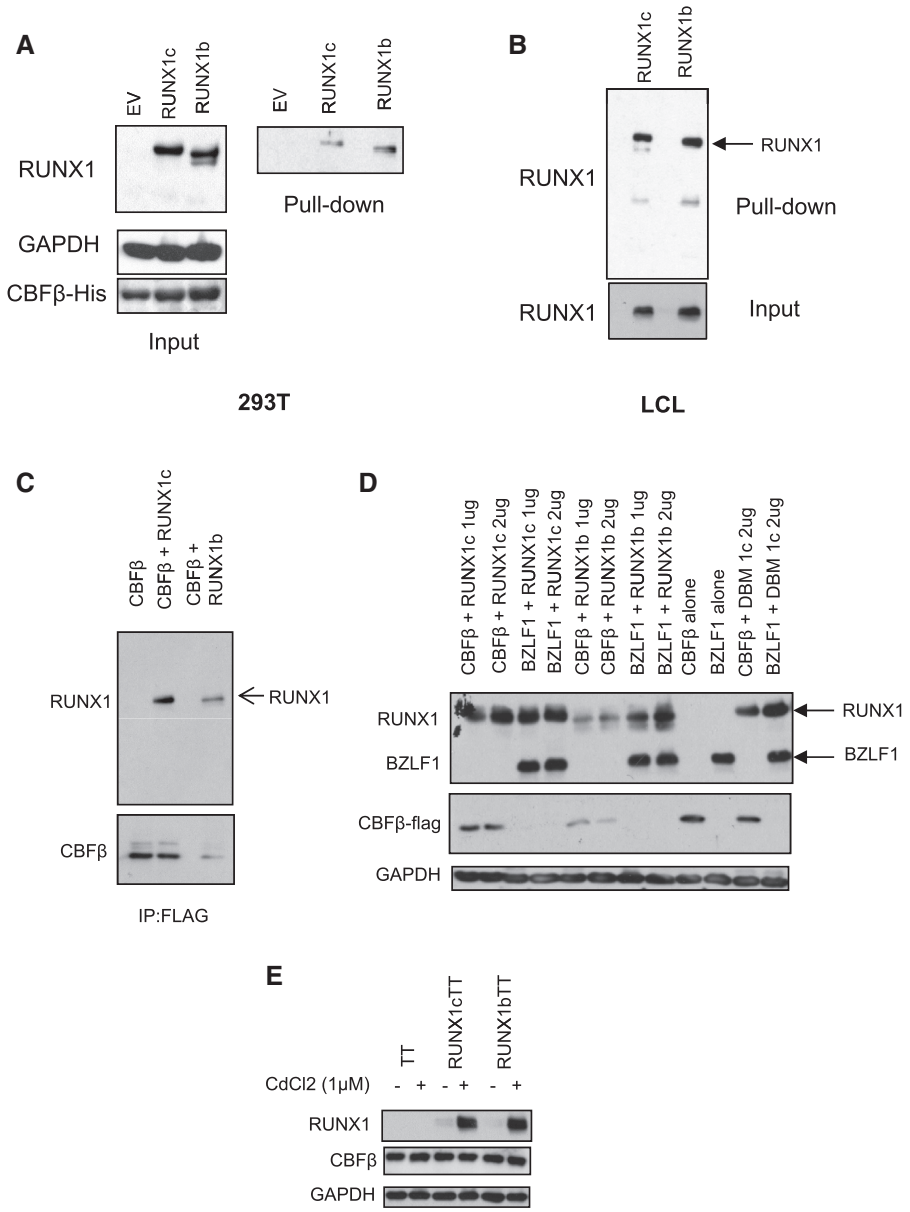


**Figure 8.** RUNX1c and RUNX1b interact equally with CBF-β. (**A**) The 10-cm dishes of HEK293T cells were transfected with 8 μg of pCEP4, pCEP–RUNX1c or pCEP–RUNX1b. Cells were lysed the following day and used for CBF-β–His protein pull-downs. A small sample of each lysate was immunoblotted for the input level of RUNX1, using GAPDH as a loading control. CBF-β–His levels on the nickel beads were assessed by staining the gel with Coomassie blue. Pull-down material was immunoblotted and probed for RUNX1. (**B**) CBF-β–His pull-downs in extracts from IB4 stable pMEP4–RUNX1cTT and RUNX1bTT induced with $CdCl_2$ showing pulled down material and lysate input probed for RUNX1 expression. (**C**) HEK293T cells were transfected with pBKCMV–CBF-β-flag alone or with pCEP–RUNX1c or pCEP–RUNX1b. Cells were lysed the following day. Anti-flag pull-downs were performed, and the material was immunoblotted and probed for RUNX1 and CBF-β-flag. (**D**) HEK293T cells were transfected with indicated plasmids, lysed the following day and immunoblotted for RUNX1 (blot re-probed with a BZLF1 antibody), FLAG and GAPDH. (**E**) IB4 pMEP4 stable cell lines expressing TT alone, RUNX1cTT or RUNX1bTT induced with 1 μM of $CdCl_2$ for 24 h. Extracts were immunoblotted to determine the effect on endogenous CBF-β levels. Data are representative of three separate experiments.

occurs during B cell activation either by EBV infection or phorbol ester treatment (15). Isoform-specific effects may thus be a key feature of RUNX biology in human B cells, and it will be important to be aware of which isoform is being expressed in studies on human cells. We propose that this phenomenon can be generalized to normal human B cell activation and that RUNX1c may contribute to the gene expression program that holds human B cells in a resting state before activation.

EBNA2, the EBV latent transcription factor that drives RUNX3 expression and, therefore, RUNX1c repression, is a functional orthologue of NotchIC, and it mimics its normal role in B cell activation (38,39). It would be interesting to examine how general this type of isoform specific effect is in other key steps during haematopoiesis. Levanon *et al.* (40) observed a dramatic decrease in RUNX1c mRNA in both whole lymphocyte preparations and the Jurkat T cell line after TPA and concanavolin

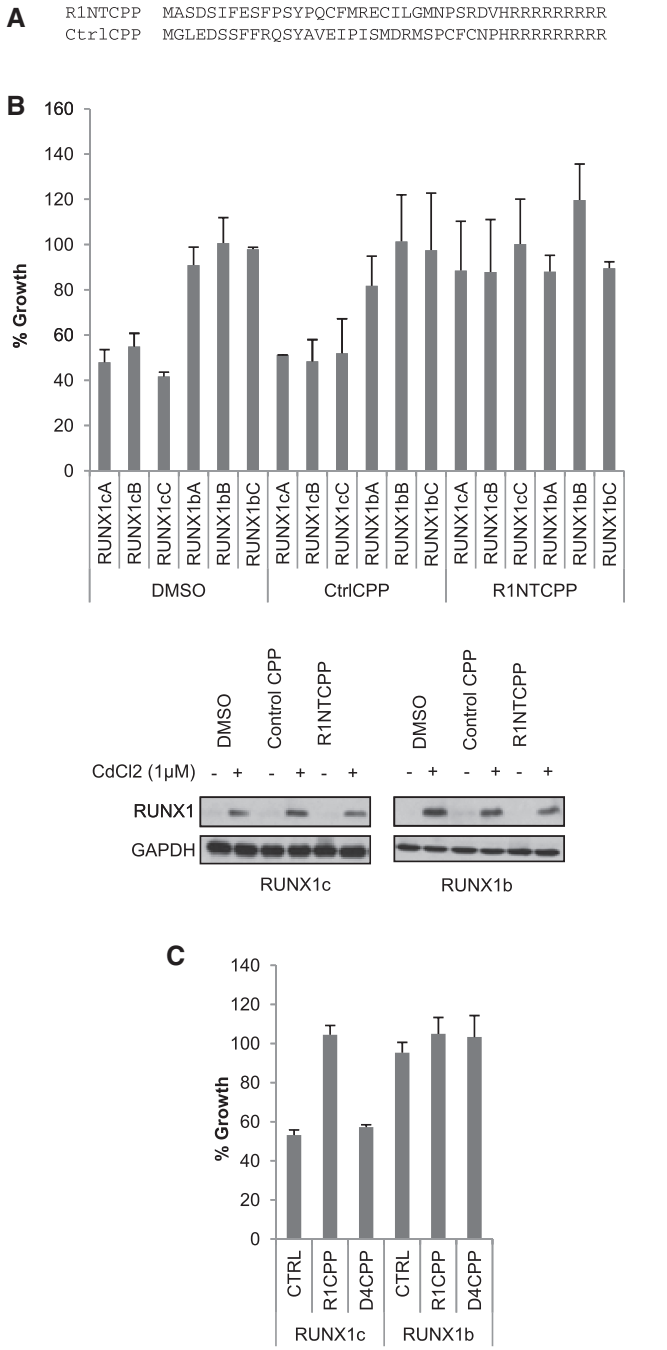


**Figure 9.** RUNX1c N-terminal cell-permeable peptide reverses growth repression. (**A**) Control scrambled and wild-type N-terminal RUNX1c CPP peptides. (**B**) Three separate clones of IB4 pMEP4–RUNX1cTT and RUNX1bTT were seeded at $1 \times 10^5$ cells per ml in six-well dishes, induced with 1 μM of $CdCl_2$ and counted after 5 days culture in the presence of DMSO, control CPP (CtrlCPP) or RUNX1c CPP (R1NTCPP). Each clone was counted three times, and the results are presented as average percentage growth of induced cells compared with non-induced cells with standard deviations shown as error bars. One clone of each cell line type was lysed and immunoblotted to determine the effect of CPPs on RUNX1 levels using GAPDH as a loading control. (**C**) The same experiment as in part B was performed using resynthesized peptides and including a RUNX1c D4A site mutant (D4CPP). Data are representative of three separate experiments.

A treatment, suggesting that this switch might also play a role in T cell activation. Other work demonstrated that overexpression of the distal but not the proximal form severely impaired thymocyte differentiation and suggested that RUNX1c must be downregulated to pass the double-negative (DN) to double-positive (DP) transition (41).

Much of the published work to date characterizing the role of RUNX1 in haematopoiesis has been conducted in mice. Some of the residues required for RUNX1c repression of LCLs reside within the exon that is absent in murine RUNX1c, resulting in absence of the critical $E^{20}$–$H^{32}$ region from mouse RUNX1c. Although human B cells do contain some spliced RNA corresponding to a murine-like form of RUNX1c N terminus (data not shown), we were unable to detect that form at the protein level. Overall, this suggests that there may be differences between mouse and human in this aspect of RUNX biology and implies that not all the mouse Runx1 data may be directly translated to the human context.

The RUNX1 fusion oncogenes TEL–RUNX1 and RUNX1–ETO were found to have different effects on cell growth in our human B cell system. TEL–RUNX1 did not inhibit LCL growth but RUNX1–ETO caused a strong inhibition of LCL growth. It is attractive to think that the absence of the N-terminal inhibitory domain from TEL–RUNX1 might contribute to its failure to inhibit B cell growth, but its cytoplasmic localization coupled with known gain-of-function contributions of the fused TEL domain in B cells are also well established determinants of its oncogenic nature. As RUNX1–ETO has a RUNX1b N-terminus, it is likely that the intolerance of LCLs for this fusion has more to do with its known adaptation to myeloid lineages than to similarities to the growth inhibitory RUNX1c activity we have described in this article.

Our deletion and mutation analysis of the N-terminal part of RUNX1c clearly shows which N-terminal amino acids are required for inhibition of B cell growth, but the detailed mechanism has not yet been identified. In addition to the N-terminus and the DNA-binding domain, RUNX1 sequences C-terminal of the RHD and unique to RUNX1 (but not the VWRPY) were also found to be required for the ability to inhibit B cell proliferation. In contrast to previous results using *in vitro* translated mouse RUNX1 (amino acids 1–190) on a murine MPO probe (13), we did not find any significant difference in specific DNA binding between RUNX1c and RUNX1b. No informative protein sequence motifs in the N-terminus of RUNX1c could be found by computer searching, and stably interacting proteins were not detected in mass spectrometry analysis comparing RUNX1c and RUNX1b. It is likely that the N-terminus of RUNX1c forms an important contact with another protein, nucleic acid or part of RUNX1c because of the ability of the RUNX1c N-terminal cell permeabilizing peptide (CPP) to block its activity. The CPP may act as a decoy to prevent association at the novel interaction interface. An alternative explanation could be that the CPP, at a higher concentration than intracellular RUNX1c, soaks up a post-translational modification that might be necessary for the growth

inhibitory effect. Whatever the explanation for its activity, this CPP represents an important novel reagent for specifically blocking RUNX1c activity and may also eventually provide a means to identify the molecular mechanism of the specific growth inhibitory effect of RUNX1c in human B cells. Furthermore, the behaviour of P1 RUNX1 alleles as dominant oncogenes in retroviral insertions (42,43) introduces the possibility of a therapeutic utility.

## ACKNOWLEDGEMENTS

Part of this work was supported by a grant from Leukaemia and Lymphoma Research.

## FUNDING

Funding for open access charge: Imperial College Trust grant.

*Conflict of interest statement*. None declared.

## REFERENCES

1. Cameron,E.R. and Neil,J.C. (2004) The Runx genes: lineage-specific oncogenes and tumor suppressors. *Oncogene*, **23**, 4308–4314.
2. de Bruijn,M.F. and Speck,N.A. (2004) Core-binding factors in hematopoiesis and immune function. *Oncogene*, **23**, 4238–4248.
3. Levanon,D. and Groner,Y. (2004) Structure and regulated expression of mammalian RUNX genes. *Oncogene*, **23**, 4211–4219.
4. Levanon,D., Bettoun,D., Harris-Cerruti,C., Woolf,E., Negreanu,V., Eilam,R., Bernstein,Y., Goldenberg,D., Xiao,C., Fliegauf,M. *et al.* (2002) The Runx3 transcription factor regulates development and survival of TrkC dorsal root ganglia neurons. *EMBO J.*, **21**, 3454–3463.
5. Levanon,D., Brenner,O., Negreanu,V., Bettoun,D., Woolf,E., Eilam,R., Lotem,J., Gat,U., Otto,F., Speck,N. *et al.* (2001) Spatial and temporal expression pattern of Runx3 (Aml2) and Runx1 (Aml1) indicates non-redundant functions during mouse embryogenesis. *Mech. Dev.*, **109**, 413–417.
6. Cai,Z., de Bruijn,M., Ma,X., Dortland,B., Luteijn,T., Downing,R.J. and Dzierzak,E. (2000) Haploinsufficiency of AML1 affects the temporal and spatial generation of hematopoietic stem cells in the mouse embryo. *Immunity*, **13**, 423–431.
7. North,T., Gu,T.L., Stacy,T., Wang,Q., Howard,L., Binder,M., Marin-Padilla,M. and Speck,N.A. (1999) Cbfa2 is required for the formation of intra-aortic hematopoietic clusters. *Development*, **126**, 2563–2575.
8. Okuda,T., van Deursen,J., Hiebert,S.W., Grosveld,G. and Downing,J.R. (1996) AML1, the target of multiple chromosomal translocations in human leukemia, is essential for normal fetal liver hematopoiesis. *Cell*, **84**, 321–330.
9. Ichikawa,M., Goyama,S., Asai,T., Kawazu,M., Nakagawa,M., Takeshita,M., Chiba,S., Ogawa,S. and Kurokawa,M. (2008) AML1/Runx1 negatively regulates quiescent hematopoietic stem cells in adult hematopoiesis. *J. Immunol.*, **180**, 4402–4408.
10. Kurokawa,M. (2006) AML1/Runx1 as a versatile regulator of hematopoiesis: regulation of its function and a role in adult hematopoiesis. *Int. J. Hematol.*, **84**, 136–142.
11. Ghozi,M.C., Bernstein,Y., Negreanu,V., Levanon,D. and Groner,Y. (1996) Expression of the human acute myeloid leukemia gene AML1 is regulated by two promoter regions. *Proc. Natl Acad. Sci. USA*, **93**, 1935–1940.
12. Pozner,A., Lotem,J., Xiao,C., Goldenberg,D., Brenner,O., Negreanu,V., Levanon,D. and Groner,Y. (2007) Developmentally regulated promoter-switch transcriptionally controls Runx1 function during embryonic hematopoiesis. *BMC Dev. Biol.*, **7**, 84.
13. Telfer,J.C. and Rothenberg,E.V. (2001) Expression and function of a stem cell promoter for the murine CBFalpha2 gene: distinct roles and regulation in natural killer and T cell development. *Dev. Biol.*, **229**, 363–382.
14. Telfer,J.C., Hedblom,E.E., Anderson,M.K., Laurent,M.N. and Rothenberg,E.V. (2004) Localization of the domains in Runx transcription factors required for the repression of CD4 in thymocytes. *J. Immunol.*, **172**, 4359–4370.
15. Spender,L.C., Cornish,G.H., Sullivan,A. and Farrell,P.J. (2002) Expression of transcription factor AML-2 (RUNX3, CBF(alpha)-3) is induced by Epstein-Barr virus EBNA-2 and correlates with the B-cell activation phenotype. *J. Virol.*, **76**, 4919–4927.
16. Spender,L.C., Whiteman,H.J., Karstegl,C.E. and Farrell,P.J. (2005) Transcriptional cross-regulation of RUNX1 by RUNX3 in human B cells. *Oncogene*, **24**, 1873–1881.
17. Brady,G., Whiteman,H.J., Spender,L.C. and Farrell,P.J. (2009) Downregulation of RUNX1 by RUNX3 requires the RUNX3 VWRPY sequence and is essential for Epstein-Barr virus-driven B-cell proliferation. *J. Virol.*, **83**, 6909–6916.
18. Ben-Bassat,H., Goldblum,N., Mitrani,S., Goldblum,T., Yoffey,J.M., Cohen,M.M., Bentwich,Z., Ramot,B., Klein,E. and Klein,G. (1977) Establishment in continuous culture of a new type of lymphocyte from a "Burkitt like" malignant lymphoma (line D.G.-75). *Int. J. Cancer*, **19**, 27–33.
19. van Santen,V., Cheung,A., Hummel,M. and Kieff,E. (1983) RNA encoded by the IR1-U2 region of Epstein-Barr virus DNA in latently infected, growth-transformed cells. *J. Virol.*, **46**, 424–433.
20. Young,L.S., Lau,R., Rowe,M., Niedobitek,G., Packham,G., Shanahan,F., Rowe,D.T., Greenspan,D., Greenspan,J.S., Rickinson,A.B. *et al.* (1991) Differentiation-associated expression of the Epstein-Barr virus BZLF1 transactivator protein in oral hairy leukoplakia. *J. Virol.*, **65**, 2868–2874.
21. Fujita,Y., Nishimura,M., Taniwaki,M., Abe,T. and Okuda,T. (2001) Identification of an alternatively spliced form of the mouse AML1/RUNX1 gene transcript AML1c and its expression in early hematopoietic development. *Biochem. Biophys. Res. Commun.*, **281**, 1248–1255.
22. Cammenga,J., Niebuhr,B., Horn,S., Bergholz,U., Putz,G., Buchholz,F., Lohler,J. and Stocking,C. (2007) RUNX1 DNA-binding mutants, associated with minimally differentiated acute myelogenous leukemia, disrupt myeloid differentiation. *Cancer Res.*, **67**, 537–545.
23. Zeng,C., van Wijnen,A.J., Stein,J.L., Meyers,S., Sun,W., Shopland,L., Lawrence,J.B., Penman,S., Lian,J.B., Stein,G.S. *et al.* (1997) Identification of a nuclear matrix targeting signal in the leukemia and bone-related AML/CBF-alpha transcription factors. *Proc. Natl Acad. Sci. USA*, **94**, 6746–6751.
24. Stifani,S., Blaumueller,C.M., Redhead,N.J., Hill,R.E. and Artavanis-Tsakonas,S. (1992) Human homologs of a Drosophila Enhancer of split gene product define a novel family of nuclear proteins. *Nat. Genet.*, **2**, 343.
25. Levanon,D., Goldstein,R.E., Bernstein,Y., Tang,H., Goldenberg,D., Stifani,S., Paroush,Z. and Groner,Y. (1998) Transcriptional repression by AML1 and LEF-1 is mediated by the TLE/Groucho corepressors. *Proc. Natl Acad. Sci. USA*, **95**, 11590–11595.
26. Schwieger,M., Lohler,J., Friel,J., Scheller,M., Horak,I. and Stocking,C. (2002) AML1-ETO inhibits maturation of multiple lymphohematopoietic lineages and induces myeloblast transformation in synergy with ICSBP deficiency. *J. Exp. Med.*, **196**, 1227–1240.
27. de Guzman,C.G., Johnson,A. and Klug,C.A. (2003) The ETO domain is necessary for the developmental abnormalities associated with AML1-ETO expression in the hematopoietic stem cell compartment *in vivo*. *Blood Cells Mol. Dis.*, **30**, 201–206.
28. Fenske,T.S., Pengue,G., Mathews,V., Hanson,P.T., Hamm,S.E., Riaz,N. and Graubert,T.A. (2004) Stem cell expression of the AML1/ETO fusion protein induces a myeloproliferative disorder in mice. *Proc. Natl Acad. Sci. USA*, **101**, 15184–15189.
29. Yuan,Y., Zhou,L., Miyamoto,T., Iwasaki,H., Harakawa,N., Hetherington,C.J., Burel,S.A., Lagasse,E., Weissman,I.L., Akashi,K. *et al.* (2001) AML1-ETO expression is directly

involved in the development of acute myeloid leukemia in the presence of additional mutations. *Proc. Natl Acad. Sci. USA*, **98**, 10398–10403.
30. Dann,E.J., Fears,S., Arad-Dann,H., Nucifora,G. and Rowley,J.D. (2000) Lineage specificity of CBFA2 fusion transcripts. *Leuk. Res.*, **24**, 11–17.
31. Morrow,M., Horton,S., Kioussis,D., Brady,H.J. and Williams,O. (2004) TEL-AML1 promotes development of specific hematopoietic lineages consistent with preleukemic activity. *Blood*, **103**, 3890–3896.
32. Kanatani,N., Fujita,T., Fukuyama,R., Liu,W., Yoshida,C.A., Moriishi,T., Yamana,K., Miyazaki,T., Toyosawa,S. and Komori,T. (2006) Cbf beta regulates Runx2 function isoform-dependently in postnatal bone development. *Dev. Biol.*, **296**, 48–61.
33. Bravo,J., Li,Z., Speck,N.A. and Warren,A.J. (2001) The leukemia-associated AML1 (Runx1)—CBF beta complex functions as a DNA-induced molecular clamp. *Nat. Struct. Biol.*, **8**, 371–378.
34. Huang,G., Shigesada,K., Ito,K., Wee,H.J., Yokomizo,T. and Ito,Y. (2001) Dimerization with PEBP2beta protects RUNX1/AML1 from ubiquitin-proteasome-mediated degradation. *EMBO J.*, **20**, 723–733.
35. Tahirov,T.H., Inoue-Bungo,T., Morii,H., Fujikawa,A., Sasaki,M., Kimura,K., Shiina,M., Sato,K., Kumasaka,T., Yamamoto,M. *et al.* (2001) Structural analyses of DNA recognition by the AML1/Runx-1 Runt domain and its allosteric control by CBFbeta. *Cell*, **104**, 755–767.
36. Koren,E. and Torchilin,V.P. (2012) Cell-penetrating peptides: breaking through to the other side. *Trends Mol. Med.*, **18**, 385–393.
37. Lysakova-Devine,T., Keogh,B., Harrington,B., Nagpal,K., Halle,A., Golenbock,D.T., Monie,T. and Bowie,A.G. (2010) Viral inhibitory peptide of TLR4, a peptide derived from vaccinia protein A46, specifically inhibits TLR4 by directly targeting MyD88 adaptor-like and TRIF-related adaptor molecule. *J. Immunol.*, **185**, 4261–4271.
38. Strobl,L.J., Hofelmayr,H., Marschall,G., Brielmeier,M., Bornkamm,G.W. and Zimber-Strobl,U. (2000) Activated Notch1 modulates gene expression in B cells similarly to Epstein-Barr viral nuclear antigen 2. *J. Virol.*, **74**, 1727–1735.
39. Hofelmayr,H., Strobl,L.J., Marschall,G., Bornkamm,G.W. and Zimber-Strobl,U. (2001) Activated Notch1 can transiently substitute for EBNA2 in the maintenance of proliferation of LMP1-expressing immortalized B cells. *J. Virol.*, **75**, 2033–2040.
40. Levanon,D., Bernstein,Y., Negreanu,V., Ghozi,M.C., Bar-Am,I., Aloya,R., Goldenberg,D., Lotem,J. and Groner,Y. (1996) A large variety of alternatively spliced and differentially expressed mRNAs are encoded by the human acute myeloid leukemia gene AML1. *DNA Cell Biol.*, **15**, 175–185.
41. Wong,W.F., Nakazato,M., Watanabe,T., Kohu,K., Ogata,T., Yoshida,N., Sotomaru,Y., Ito,M., Araki,K., Telfer,J. *et al.* (2010) Over-expression of Runx1 transcription factor impairs the development of thymocytes from the double-negative to double-positive stages. *Immunology*, **130**, 243–253.
42. Stewart,M., Terry,A., Hu,M., O'Hara,M., Blyth,K., Baxter,E., Cameron,E., Onions,D.E. and Neil,J.C. (1997) Proviral insertions induce the expression of bone-specific isoforms of PEBP2alphaA (CBFA1): evidence for a new myc collaborating oncogene. *Proc. Natl Acad. Sci. USA*, **94**, 8646–8651.
43. Wotton,S., Stewart,M., Blyth,K., Vaillant,F., Kilbey,A., Neil,J.C. and Cameron,E.R. (2002) Proviral insertion indicates a dominant oncogenic role for Runx1/AML-1 in T-cell lymphoma. *Cancer Res.*, **62**, 7181–7185.